ORIGINAL PAPER

CrossMark

Magnetite nanoparticles coated with mercaptosuccinic acid-modified mesoporous titania as a hydrophilic sorbent for glycopeptides and phosphopeptides prior to their quantitation by LC-MS/MS

Nianrong Sun[1] · Jiawen Wang[1] · Jizong Yao[1] · Hemei Chen[1] · Chunhui Deng[1,2]

Abstract

A hydrophilic material consisting of a magnetite core coated with mercaptosuccinic acid modified mesoporous titania (denoted as $Fe_3O_4@mTiO_2$-MSA) has been fabricated. It is shown to be a viable sorbent for capturing glycopeptides and phosphopeptides. The sorbent combines the features of metal oxide-based affinity chromatography and of hydrophilic interaction liquid chromatography (HILIC) with the advantages of using mesoporous titania. The use of magnetic microspheres provides magnetic response and simplifies separation. Following elution with 10% ammonia, the peptides were submitted to LC-MS/MS analysis. The method enabled 327 phosphopeptides and 65 glycopeptides to be identified in three isolated replicates of merely 5 μL samples of human saliva. Among them, the phosphorylation sites and glycosylation sites were detected in 20 peptide segments.

Introduction

Different types of post-translational modifications (PTMs) endow the proteins with more perfect functions and more precise regulation ability so that organism can regulate complex physiological processes in the case of a limited number of genes [1]. Glycosylation and phosphorylation, both of which have significant biological effects on structure and function of proteins, are widely recognized to be common and prominent [2–6]. Studies show that alternation or abnormity of glycosylation/phosphorylation have a direct connection with many diseases especially for neurological disorders and cancers [7–9]. And the research for glycosylation/phosphorylation is crucial for discovering potential biomarkers connected with diseases. Moreover, various PTM processes in organism are not isolated but mutually coordinated and interplayed. A great many reports have put forward powerful evidences for the interaction effects between glycosylation and phosphorylation [10–12]. For instance, Gong et al. reported that the tau glycosylation might facilitate its abnormal hyperphosphorylation in Alzheimer's disease (AD) brains [13]. Thus, it is seriously necessary to carry out researches on simultaneous analysis of glycosylation and phosphorylation, which may make great contribution to clarify their relationship in disease pathology. Moreover, it may be beneficial to sequentially discover potential biomarkers easier for early diagnosis of diseases, or develop new drugs and so forth.

In PTM proteomics research, although mass spectrometry (MS) technique developed rapidly because of its high throughput and high sensitivity, high-efficient separation. The enrichment of PTM proteins is essential prior to MS analysis because of the high complexity of bio-samples and low abundance of targets, etc. [14–17]. Up to now, series of good strategies have been developed to enrich glycopeptides or phosphopeptides, respectively. For phosphopeptides enrichment, immobilized metal ion

✉ Chunhui Deng
chdeng@fudan.edu.cn

[1] Department of Chemistry and The Fifth People's Hospital of Shanghai, Fudan University, Shanghai 200433, China

[2] Institutes of Biomedical Sciences and Collaborative Innovation Center of Genetics and Development, Fudan University, Shanghai 200433, China

affinity chromatography (IMAC) [18–21] and metal oxide affinity chromatography (MOAC) [22–24] are two most widely used methods. It has been demonstrated that both of them possess excellent enrichment performance for phosphoproteomics research. According to reports [25, 26], metal oxide microspheres such as TiO_2 perform better in capturing phosphopeptides than conventional IMAC because they can reduce nonspecific binding, and the reproducibility of results are better. Mesoporous metal oxide microspheres have a larger specific surface than nonporous ones. Hence, they offer more binding sites that results in higher enrichment capacity. In addition, there are also two well investigated ways for glycopeptides enrichment: one is boronic acid chemistry [27–29], which depends on the reversible binding ability between boronic acids and cis-diols. However, real-world applications of boronic acid chemistry often face three challenges such as weak affinity, non-biocompatible binding pH and the problems in selectivity manipulation. The other is hydrophilic interaction chromatography (HILIC) [30–33] which takes advantages of better hydrophilicity of N-glycopeptides compared with non-glycosylated peptides. As a result, HILIC strategy exhibits a variety of merits such as unbiased enrichment performance towards glycopeptides with various glycoforms, high-efficient enrichment capacity, good reproducibility, good compatibility with MS analysis etc.

Herein, for the first time, we designed and fabricated a specific sorbent, viz. hydrophilic mercaptosuccinic acid (MSA) coupled magnetic mesoporous titania (dubbed $Fe_3O_4@mTiO_2$-MSA). The sorbent combines different advantages, which included the above described advantages of MOAC and HILIC and rapid magnetic responsiveness, as well as the merits of mesoporous titania such as large surface area for high load capacity to carry functional molecules. MSA, which often serves as capping agent for preparation of gold particles or quantum dots to improve their hydrophilicity [34], was immobilized on the mesoporous titania shell by taking advantages of interaction between titanium and thiol groups, thereby rendering the mesoporous titania with outstanding hydrophilicity. Human saliva [35], which is considered as an ideal clinic specimen on account of noninvasive collection, has been gaining increasing attention. Therefore, we chose human saliva as complicated biosamples to test the performance of $Fe_3O_4@mTiO_2$-MSA for simultaneous enrichment of glycopeptides and phosphopeptides. Indeed, the specific sorbent exhibits highly specific and efficient simultaneous adsorption ability for glycopeptides and phosphopeptides.

Experimental

Materials and reagents

Tetrabutyl titanate (TBOT, #244112), ammonium bicarbonate (NH_4HCO_3, #09830), horseradish peroxidase (HRP,

#P8375), β-casein (#C6905), bovine serum albumin (BSA, #A1933), Immunoglobulin G (IgG, #56834), dithiothreitol (DTT, #43815), iodoacetamide (IAA, #I1149), trifluoroacetic acid (TFA, #302031) and 2,5-dihydroxybenzoic acid (DHB, #85707) were purchased from Sigma-Aldrich (USA, https://www.sigmaaldrich.com). Mercaptosuccinic acid (MSA, #78172) was purchased from Adamas-beta (http://www.adamas-beta.com). Concentrated ammonia solution (28 wt%, #10002108) were purchased from Sinopharm Chemical Reagent Co., Ltd. (https://www.reagent.com.cn/). PNGase F (#P0705s) was purchased from Genetimes Technology (http://www.genetimes.com.cn/). Acetonitrile (ACN, #1.00029.2500) of chromatographically pure was purchased from Merck (Darmstadt, Germany, https://www.merckgroup.com/cn-zh). All deionized water in the experiment are acquired by Milli-Q system (Millipore, Bedford, MA). All of other chemicals are analytically pure. Saliva samples were provided by healthy woman.

Synthesis of mercaptosuccinic acid modified mesoporous titania on magnetite nanoparticles ($Fe_3O_4@mTiO_2$-MSA)

The procedures for synthesis of the specific dual functional sorbent are displayed in Fig. 1. Briefly, the Fe_3O_4 was prepared by utilizing our previous method [27]. Fe_3O_4 nanoparticles (80 mg) were dispersed in 200 mL of ethanol containing 0.72 mL ammonia solution (28 wt%) with the help of ultrasonication for 15 min. The mixture was then mechanically stirred for 5 min before 1.6 mL titania precursor, TBOT, was added in drops, and continuously stirred at 45 °C for 24 h. The particles were washed with deionized water and ethanol for several times and then dispersed into a mixture of 40 mL ethanol and 20 mL deionized water. The dispersion was transferred into stainless-steel autoclave and heated at 80 °C for 12 h. The nanoparticles were calcined at 400 °C for 2 h to improve crystallinity (denoted as $Fe_3O_4@mTiO_2$). Finally, $Fe_3O_4@mTiO_2$ nanoparticles (20 mg) and mercaptosuccinic acid (MSA, 10 mg) were dispersed in ethanol (20 mL) by ultrasonication and continuously stirred at room temperature overnight. The dual functional sorbent (denoted as $Fe_3O_4@mTiO_2$-MSA) were washed with ethanol for three times and dried in vacuum overnight for the following experiments.

Preparation of standard protein digests

Standard protein (β-casein, HRP or IgG, 2 mg) was dissolved in NH_4HCO_3 (1 mL, 25 mmol·L^{-1}, pH = 7.9) and denatured at 95 °C for 10 min. Once cooling down to room temperature, the solution was treated with trypsin (protein/Trypsin = 40/1,

Fig. 1 Schematic diagram of the preparation of Fe$_3$O$_4$@mTiO$_2$-MSA to enrich glycopeptides and phosphopeptides
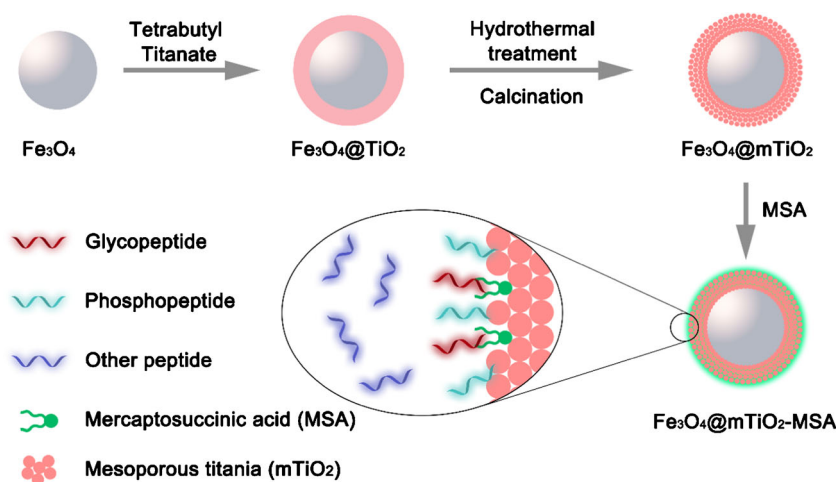
w/w) proceeding digestion at 37 °C for 16 h. For BSA, the adding amount was 10 mg and other steps were the same as the previous description.

Preparation of human saliva samples

Human saliva was taken from a healthy female volunteer according to the reported method [36]. Briefly, an equal volume of 0.2% TFA solution was mixed with the saliva sample, deposit of which was removed via centrifugation. The final sample was stored at −80 °C for the following experiments.

Characterization

The TEM images of the specific dual functional sorbent were acquired by JEOL 2011 transmission electron microscopy. Micromeritcs Tristar 3000 analyzer was employed to the measurement of nitrogen sorption isotherms. X-ray photoelectron spectroscopy (XPS) pattern were adopted by ESCALab220i-XL electron spectrometer (VG Scientific) using 300 W Al Kα radiation. The base pressure was about 3×10^{-9} mbar. The binding energies were referenced to C 1 s line at 284.8 eV from adventitious carbon. All MALDI-TOF MS experiments were performed on AB Sciex 5800 MALDI TOF/TOFTM mass spectrometer (AB Sciex, USA) in a reflector positive mode with a 355 nm Nd-YAG laser, 200 Hz frequency, and acceleration voltage of 20 kV.

## Enrichment protocols for glycopeptides and phosphopeptides

For phosphopeptides, Fe$_3$O$_4$@mTiO$_2$-MSA (100 μg) was added into loading buffer (ACN/H$_2$O/TFA = 50/49.9/0.1, v/v/v, 100 μL) containing β-casein digests (1×10^{-7} mol·L^{-1}). The suspension was incubated at 37 °C for 20 min.

After separated by magnet, Fe$_3$O$_4$@mTiO$_2$-MSA was washed with loading buffer (3×200 μL) and the phosphopeptides were eluted with ammonia solution (10 μL, 0.4 mol·L^{-1}) for 20 min. Finally, the eluent was mixed with matrix solution for further MALDI-TOF MS analysis.

For glycopeptides enrichment, Fe$_3$O$_4$@mTiO$_2$-MSA (100 μg) was added into loading buffer (ACN/H$_2$O/TFA = 90/7/3, v/v/v, 100 μL) with HRP or IgG digests (1×10^{-7} mol·L^{-1}). The suspension was incubated at 37 °C for 20 min and consequently separated by magnet, followed by washing with loading buffer (3×200 μL) to remove non-glycosylated peptides. The glycopeptides were eluted with ACN/H$_2$O/TFA (50/49/1, /v/v/v, 8 μL) at 37 °C for 20 min. At last, the eluent was mixed with matrix solution for MALDI-TOF MS analysis.

For simultaneous enrichment of phosphopeptides and glycopeptides from standard samples, Fe$_3$O$_4$@mTiO$_2$-MSA (150 μg) was added into loading buffer (ACN/H$_2$O/TFA = 90/7/3, v/v/v, 100 μL) with the mixture of β-casein and HRP digestion (1×10^{-7} mol·L^{-1}). The suspension was incubated at 37 °C for 30 min. After separated from supernatant with applied magnetic field, Fe$_3$O$_4$@mTiO$_2$-MSA was washed with loading buffer (3×200 μL). The phosphopeptides and glycopeptides were then eluted with ammonia solution (10%,10 μL) for 30 min. The eluent was mixed with matrix solution for MALDI-TOF MS analysis.

For one-step enrichment of phosphopeptides and glycopeptides from saliva samples, saliva (5 μL) was dispersed in 95 μL loading buffer (ACN/H$_2$O/TFA = 90/7/3, v/v/v) which contains 300 μg Fe$_3$O$_4$@mTiO$_2$-MSA. The enrichment proceeded at 37 °C for 40 min and was subsequently washed with 100 μL loading buffer for four times. The enriched glycopeptides and phosphopeptides were eluted by 10% ammonia solution (30 μL) for twice and then lyophilized for the subsequent deglycosylation step.
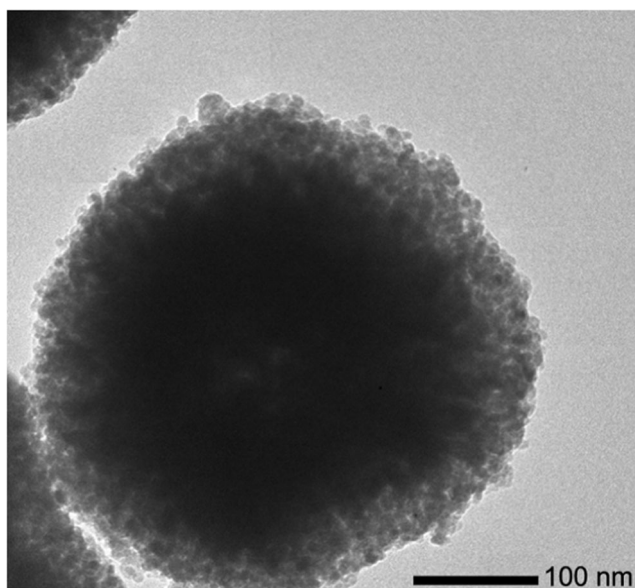
Fig. 2 The TEM image of Fe$_3$O$_4$@mTiO$_2$-MSA sorbent

Results and discussion

Preparation and characterization of Fe$_3$O$_4$@mTiO$_2$-MSA

The synthetic procedure is displayed in Fig. 1. Briefly, Fe$_3$O$_4$@TiO$_2$ was easily synthesized by the hydrolysis and condensation of titania precursor, TBOT, on the magnetic nanoparticles. With hydrothermal treatment and calcination at 400 °C for 2 h, Fe$_3$O$_4$@mTiO$_2$ core-shell microspheres were obtained. Finally, the Fe$_3$O$_4$@mTiO$_2$-MSA was synthesized via the interaction of sulfhydryl group of mercaptosuccinic acid and titania.

The morphology of the specific sorbent was firstly characterized by transmission electron microscopy (TEM), which demonstrated that the Fe$_3$O$_4$ magnetic nanoparticles were well-encapsulated in mesoporous titania shell and the mean diameter is about 400 nm (Fig. 2). Besides, a representative type-IV isotherm with hysteresis loop corresponding to mesoporous nanomaterials was obtained through Brunauer-Emmett-Teller (BET) gas sorptometry measurement (Fig. S1A). The BET surface area of Fe$_3$O$_4$@mTiO$_2$-MSA was calculated to be 106.9 m$^2 \cdot$g^{-1} and the total pore volume was about 0.271 cm$^3 \cdot$g^{-1}. From Fig. S1B, the pore-size distribution calculated by Barrett-Joyner-Halenda (BJH) method indicates the average pore size is about 6.7 nm. This result demonstrates the successful formation of magnetic mesoporous titania microspheres. Fig. S2 shows that the sorbent can be well dispersed and rapidly separated from water by using an external magnet.

The energy dispersive X-ray (EDX) analysis was applied to determine the existence of C, O, S, Ti, Fe and Cu in the specific functional sorbent (Fig. S3, the Cu peaks were from the copper grid for TEM). Preliminarily, it confirms the successful immobilization of mercaptosuccinic acid on the specific sorbent. Additionally, X-ray photoelectron spectroscopy (XPS) was employed to investigate the surface elements of MSA functionalized magnetic mesoporous titania nanoparticles. As shown in Fig. S4, evident peaks of Fe 2p, Ti 2p3, Ti 3p, C 1 s, O 1 s and S 2p3 are observed. The Ti 2p3/2–1/2 peak was studied by peak-differenating analysis (Fig. S4B) where it seems obviously that the doublets are made up of Ti-O bond and Ti-S bond (Binding energy is listed in Table S1). It directly indicates that the immobilization of mercaptosuccinic acid is based on the interaction between titania and the thiol group of MSA. Afterwards, loading amount of mercaptosuccinic acid was determined by
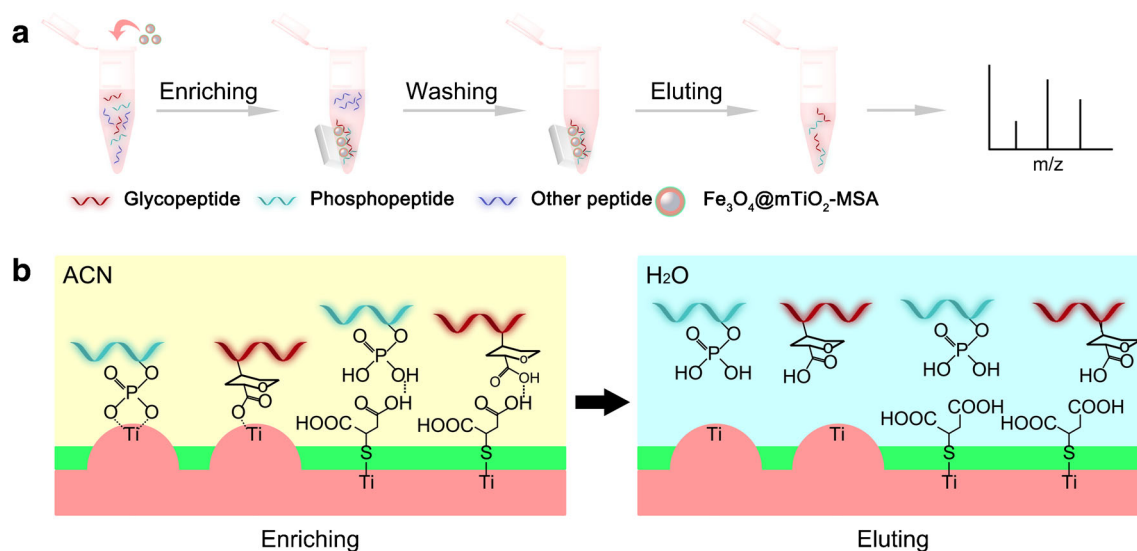
Fig. 3 **a** Flowchart of the enrichment process with the Fe$_3$O$_4$@mTiO$_2$-MSA sorbent; **b** Binding modes of between (sialic acid-containing) glycopeptides/phosphopeptides and functional groups of Fe$_3$O$_4$@mTiO$_2$-MSA in different conditions

thermogravimetric Analysis (TGA). As seen in Fig. S5, no obvious weight loss can be observed in the curve of $Fe_3O_4@mTiO_2$ microspheres, demonstrating their excellent thermal stability under high temperature. However, for the curve of $Fe_3O_4@mTiO_2$-MSA, apparent mass loss can be seen after 200 °C, and thus the loading amount of MSA on $Fe_3O_4@mTiO_2$ is calculated to be about 12.6 wt%.

Individual enrichment of N-glycopeptides and phosphopeptides from standard proteins by $Fe_3O_4@mTiO_2$-MSA

As seen in Fig. 3, the enrichment procedure and the potential binding modes between different glycopeptides/

phosphopeptides and $Fe_3O_4@mTiO_2$-MSA are briefly illustrated in Fig. 3a and Fig. 3b, respectively. Considering the successful modification of MSA, the enrichment performance of $Fe_3O_4@mTiO_2$-MSA for N-glycopeptides were firstly tested by choosing horseradish peroxidase (HRP) digestion as standard sample. As shown in Fig. 4, only 3 weak glycopeptide peaks with strong interference are detected by direct MS analysis of HRP digest. However, after enrichment by $Fe_3O_4@mTiO_2$-MSA, 22 enhanced signals corresponding to glycopeptides are detected by MALDI-TOF MS (Fig. 4b, detailed information is listed at Table S2). The excellent enrichment performance of $Fe_3O_4@mTiO_2$-MSA towards glycopeptides should be attributed to good hydrophilic property of immobilized MSA. Even if the concentration of HRP digest

Fig. 4 MALDI-TOF MS of 1 × 10^{-7} mol·L^{-1} HRP digest and 1 × 10^{-7} mol·L^{-1} β-casein digest [(**a**, **c**) before enrichment (**b**, **d**) enriched by $Fe_3O_4@mTiO_2$-MSA]. Glycopeptides from HRP digest are marked with ⬤, phosphopeptides from β-casein digest are marked with "*" and dephosphorylated fragments are marked with "#"
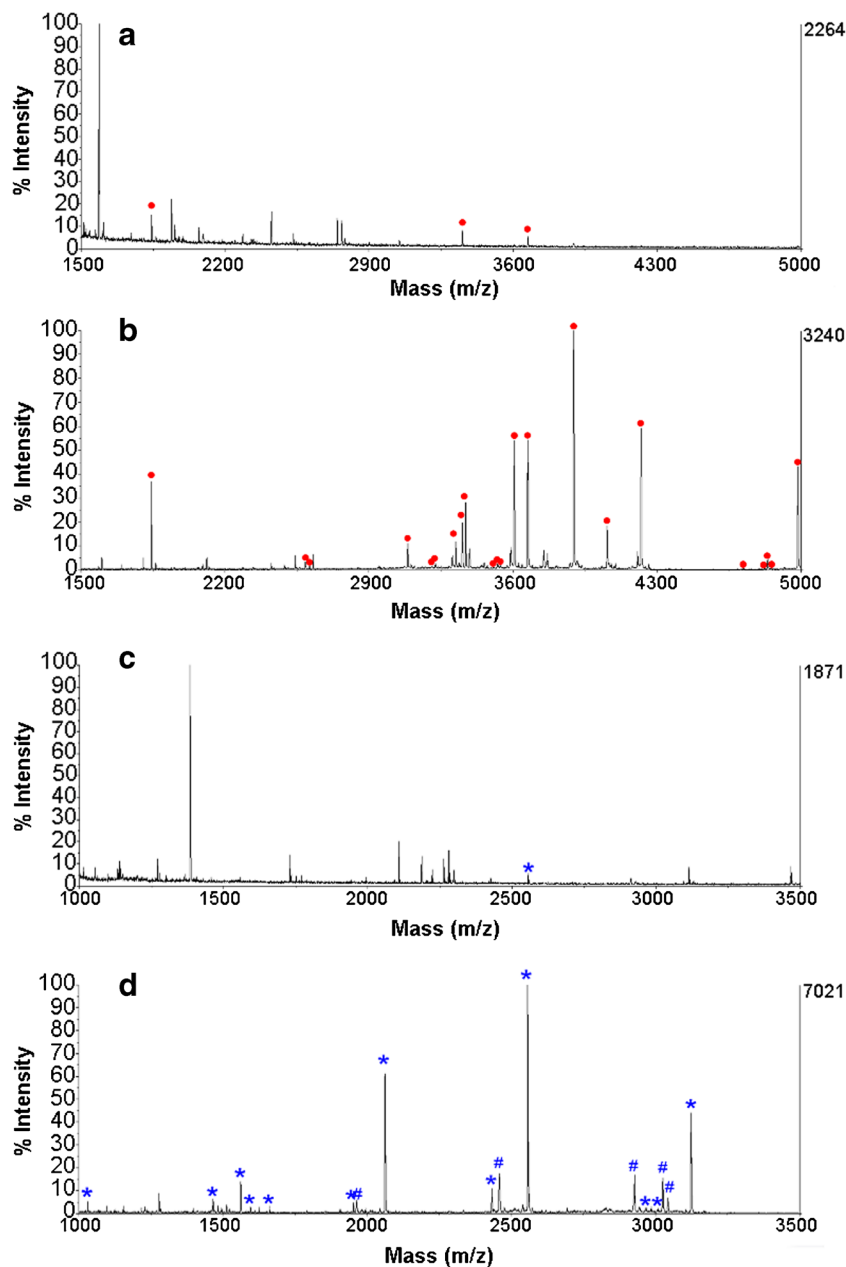
is decreased to 1×10^{-9} mol·L^{-1}, six glycopeptides still can be detected as shown in Fig. S7B, which is competitive to previous reports (Table S3). Also, sialic acid-containing glycopeptides (IgG digest) are employed to determine the enrichment performance of Fe$_3$O$_4$@mTiO$_2$-MSA, since IgG has different kinds of glycoforms from HRP. After enrichment with Fe$_3$O$_4$@mTiO$_2$-MSA, 26 enhanced glycopeptides peaks can be clearly observed in Fig. S6, while no detectable glycopeptides peaks appear in the MS spectra before enrichment (detailed information is listed at Table S4). This result suggests the unbiased enrichment capacity of Fe$_3$O$_4$@mTiO$_2$-MSA towards glycopeptides with different glycoforms. The binding capacity of Fe$_3$O$_4$@mTiO$_2$-MSA for N-glycopeptides is calculated to be 150 mg·g^{-1} (Fig. S8), which can be owed to the existence of big mesopores. Furthermore, digestion of typical non-glycosylated and non-phosphorylated protein-bovine serum albumin (BSA) are employed to investigate the enrichment selectivity of Fe$_3$O$_4$@mTiO$_2$-MSA for glycopeptides. From Fig. S9A, it can be clearly observed that a large number of strong BSA peptides peaks dominate the MS spectra in the direct analysis of peptides mixture of HRP and BSA (1:100, w/w), while no detectable glycopeptides can be seen in the

spectra. After enrichment, twenty glycopeptides with strong intensity can be detected (Fig. S9E), indicating Fe$_3$O$_4$@mTiO$_2$-MSA has outstanding selective enrichment capacity towards glycopeptides.

Besides, in view of the presence of mesoporous titania, the enrichment ability of Fe$_3$O$_4$@mTiO$_2$-MSA for phosphopeptides is also evaluated. In this part, tryptic digestion of common phosphorylated proteins (β-casein) was chosen as the standard sample. From Fig. 4c, only one weak phosphopeptide peak is detected in the direct analysis of β-casein digest. However, after enrichment by Fe$_3$O$_4$@mTiO$_2$-MSA, seventeen peaks with significantly increased intensity are detected and attributed to phosphopeptides from both of β-casein and α-casein. Among much else eleven peaks are from β-casein, and the others belonged to the unavoidable contaminated protein (α-casein) in commercial β-casein samples (Fig. 4d, detailed information is listed at Table S5). The limit of detection of Fe$_3$O$_4$@mTiO$_2$-MSA is low as 5×10^{-11} mol·L^{-1} (Fig. S7) and binding capacity, calculated by decreasing the dosage of Fe$_3$O$_4$@mTiO$_2$-MSA, is up to 200 mg/g (Fig. S8). Similarly, β-casein digests are mixed with BSA digest at mass ratios of 1:100, 1:400 and 1:800 to evaluate the enrichment selectivity of Fe$_3$O$_4$@mTiO$_2$-MSA for

Fig. 5 MALDI-TOF MS spectra of 1×10^{-7} mol·L^{-1} HRP and β-casein digests: **a** before enrichment **b** enriched by Fe$_3$O$_4$@mTiO$_2$ microspheres **c** enriched by Fe$_3$O$_4$@mTiO$_2$-MSA sorbent. Glycopeptides from HRP digest are marked with ●, phosphopeptides from β-casein digest are marked with "*" and dephosphorylated fragments are marked with "#"
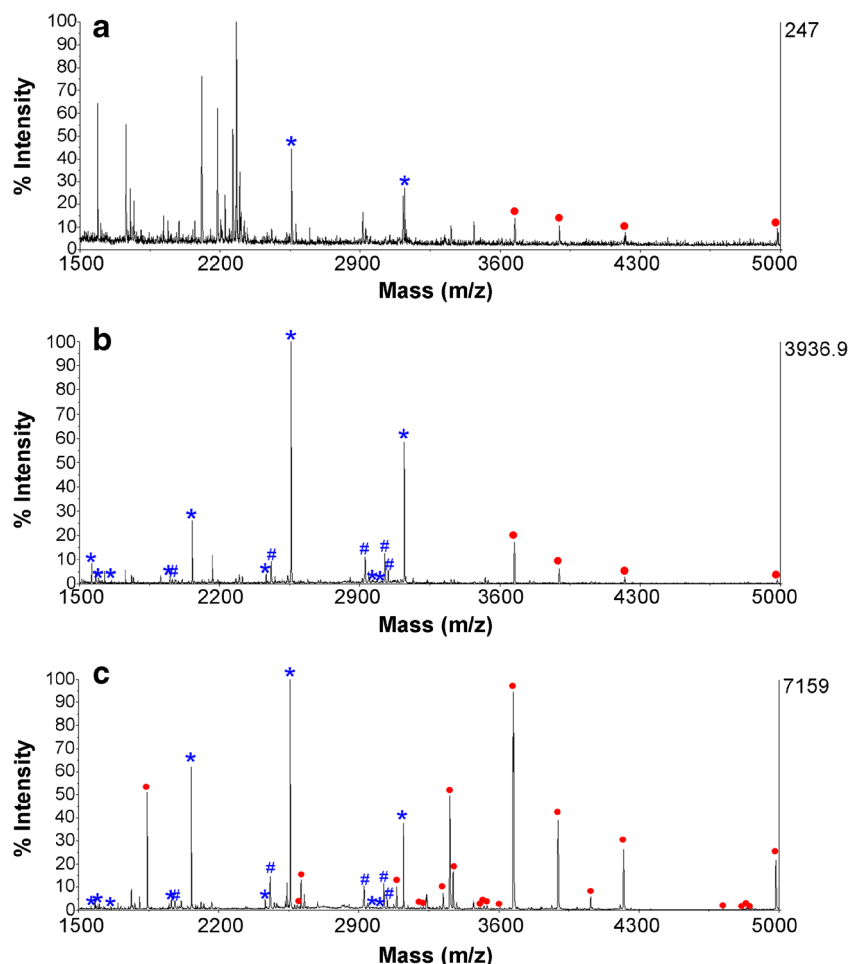
phosphopeptides. As shown in Fig. S9, fifteen phosphopeptides with clear background are detected by MALDI-TOF MS after enrichment, while only strong BSA peptides peaks can be observed before. Even with the increasing interference from the added BSA peptides, little change in number and intensity of these phosphopeptides peaks is detected. All these results indicate the outstanding enrichment specificity of the multifunctional sorbent towards phosphopeptides.

Simultaneous enrichment of N-glycopeptides and phosphopeptides by Fe$_3$O$_4$@mTiO$_2$-MSA

Encouraged by the above results, the simultaneous enrichment ability of Fe$_3$O$_4$@mTiO$_2$-MSA for both glycopeptides and phosphopeptides arouses our great interest, and thereby is tested. At first, the simultaneous enrichment conditions are investigated to make the enrichment procedure more efficient and provide more significant information in deep analysis of minute biological samples. The incubation condition of Fe$_3$O$_4$@mTiO$_2$-MSA was evaluated by capturing phosphopeptides and glycopeptides at the same time from the mixture of β-casein and HRP digestion. With the increasing proportion of acetonitrile, more glycopeptides with enhanced intensities and clear background are identified (Fig. S10). Finally, 90% ACN/3% TFA is chosen as loading buffer for simultaneous enrichment procedure.

After optimizing the incubation conditions, a total of 15 phosphopeptides and 22 glycopeptides with clear background are detected by MS (Fig. 5c). For comparison, Fe$_3$O$_4$@mTiO$_2$ microspheres were also applied to simultaneous capture of phosphopeptides and glycopeptides. Although Fe$_3$O$_4$@mTiO$_2$ microspheres perform well in the enrichment of phosphopeptides, only few glycopeptide peaks are observed in Fig. 5. This result confirms that the outstanding glycopeptides enrichment capacity of Fe$_3$O$_4$@mTiO$_2$-MSA is based on the successful immobilization of MSA. Moreover, Fe$_3$O$_4$@mTiO$_2$-MSA was stored in −20 °C for five weeks to evaluate its stability. As shown in Fig. S11, the number and peak intensities of phosphopeptides and glycopeptides basically keep stable compared with the newly synthesized one, indicating good stability of Fe$_3$O$_4$@mTiO$_2$-MSA.

Inspired by the excellent enrichment capacity and selectivity of the specific sorbent, we further apply them to enrich phosphorylated and glycosylated peptides from complex biological samples. Human saliva, which contains abundant indigenous peptides, provides lots of potential values for diseases diagnosis or monitoring therapeutic efficacy. Hence, the specific sorbent was employed in simultaneous analysis of phosphopeptides and glycopeptides by taking healthy human saliva as samples. After enriched by Fe$_3$O$_4$@mTiO$_2$-MSA, N-linked glycans are removed by PNGase F for Nano LC-MS/MS analysis. In total, there are 307 unique phosphopeptides and 65 glycopeptides identified from three isolated replicates of merely 5 μL saliva (detailed information for sites is listed in Table S6). And more importantly, 20 of them were identified having both of glycosylation site and phosphorylation site. All these results mentioned above suggest that this novel sorbent exhibit excellent simultaneous enrichment performance from both standard protein digestions and complicated biological samples, and is promising in large-scale analysis of glycopeptides and phosphopeptides. The detailed comparative information with other reports is displayed in Table S3. One of the biggest advantages of Fe$_3$O$_4$@mTiO$_2$-MSA is that it is potential in extraction of other biomolecules with phosphate groups or hydrophilic peptide/molecules, which will inspire other researchers to apply this sorbent in wider fields. However, this sort of advantage also leads to a relatively poor the selectivity compared to other specific strategies such as antibody.

Conclusion

A novel specific sorbent for simultaneous capture and profiling of glycopeptides and phosphopeptides has been developed and applied to standard protein digestion and biological samples with various merits such as high sensitivity and excellent selectivity. The outstanding enrichment performance of the sorbent largely depends on the large surface area, excellent hydrophilicity of immobilized MSA, interaction between titania and phosphate groups and strong magnetic response. Finally, a total of 307 phosphopeptides and 65 glycopeptides are identified from healthy human saliva. The outstanding simultaneous enrichment capacity makes it a powerful tool for deep analysis of glycoproteomics and phosphoproteomics and shows promise in discoveries of disease biomarkers and pathology.

Compliance with ethical standards   The author(s) declare that they have no competing interests.

References

1.   Mann M, Jensen ON (2003) Proteomic analysis of post-translational modifications. Nat Biotechnol 21(3):255–261

2.   Drickamer K, Taylor ME (1998) Evolving views of protein glycosylation. Trends Biochem Sci 23(9):321–324

3.   Kontou M, Weidemann W, Bork K, Horstkorte R (2009) Beyond glycosylation: sialic acid precursors act as signaling molecules and are involved in cellular control of differentiation of PC12 cells. Biol Chem 390(7):575–579

4. Bajaj SO (2015) A de novo approach towards glycosylation using iterative Pd-/B-dual catalysis: applications in natural products synthesis, digitoxin analogues, oligomannose motifs and their SAR studies. J Appl Phys 76(10):5760–5763

5. Dominik E, Lena H, Khoa PT, Christopher B, Qiu W, Wright PC, Sonja-Verena A, Bettina S (2016) Protein phosphorylation and its role in archaeal signal transduction. FEMS Microbiol Rev 40(5): 625–647

6. Haystead TAJ, Sim ATR, Carling D, Honnor RC, Tsukitani Y, Cohen P, Hardie DG (1989) Effects of the tumour promoter okadaic acid on intracellular protein phosphorylation and metabolism. Nature 337(6202):78–81

7. Mi K, Johnson GV (2006) The role of tau phosphorylation in the pathogenesis of Alzheimer's disease. Curr Alzheimer Res 3(5):449–463

8. Muntané G, Dalfó E, Martinez A, Ferrer I (2008) Phosphorylation of tau and alpha-synuclein in synaptic-enriched fractions of the frontal cortex in Alzheimer's disease, and in Parkinson's disease and related alpha-synucleinopathies. Neuroscience 152(4):913–923

9. Guerry P (1997) Nonlipopolysaccharide surface antigens of campylobacter species. J Infect Dis 176(2):122–124

10. Lefebvre T, Ferreira S, Dupont-Wallois L, Bussière T, Dupire M-J, Delacourte A, Michalski J-C, Caillet-Boudin M-L (2003) Evidence of a balance between phosphorylation and O-GlcNAc glycosylation of tau proteins—a role in nuclear localization. BBA-Gen Subjects 1619(2):167–176

11. Robertson LA, Moya KL, Breen KC (2004) The potential role of tau protein O-glycosylation in Alzheimer's disease. J Alzheimers Dis 6(5):489–495

12. Del Grosso F, De Mariano M, Passoni L, Luksch R, Tonini GP, Longo L (2011) Inhibition of N-linked glycosylation impairs ALK phosphorylation and disrupts pro-survival signaling in neuroblastoma cell lines. BMC Cancer 11:525

13. Liu F, Zaidi T, Iqbal K, Grundke-Iqbal I, Merkle RK, Gong C-X (2002) Role of glycosylation in hyperphosphorylation of tau in Alzheimer's disease. FEBS Lett 512:101–106

14. Zhang H, Guo T, Li X, Datta A, Park JE, Yang J, Lim SK, Tam JP, Sze SK (2010) Simultaneous characterization of glyco- and phosphoproteomes of mouse brain membrane proteome with electrostatic repulsion hydrophilic interaction chromatography. Mol Cell Proteomics 9(4):635–647

15. Zou X, Jie J, Yang B (2017) Single-step enrichment of N-Glycopeptides and Phosphopeptides with novel multifunctional Ti4+-immobilized dendritic Polyglycerol coated chitosan Nanomaterials. Anal Chem 89(14):7520–7526

16. Wang X-D, Liu Y-J, Li F-J, Li Z-L (2017) Poplar catkin: a natural biomaterial for highly specific and efficient enrichment of sialoglycopeptides. Chin Chem Lett 28(5):1018–1026

17. Wu Z, Xu N, Li W, Lin J-M (2019) A membrane separation technique for optimizing sample preparation of MALDI-TOF MS detection. Chin Chem Lett 30(1):95–98

18. Liu M, Tran TM, Abbas Elhaj AA, Bøen Torsetnes S, Jensen ON, Sellergren B, Irgum K (2017) Molecularly imprinted porous monolithic materials from melamine–formaldehyde for selective trapping of Phosphopeptides. Anal Chem 89(17):9491–9501

19. Yan Y, Zheng Z, Deng C, Li Y, Zhang X, Yang P (2013) Hydrophilic Polydopamine-coated Graphene for metal ion immobilization as a novel immobilized metal ion affinity chromatography platform for Phosphoproteome analysis. Anal Chem 85(18): 8483–8487

20. Jiang J, Sun X, She X, Li J, Li Y, Deng C, Duan G (2018) Magnetic microspheres modified with Ti(IV) and Nb(V) for enrichment of phosphopeptides. Microchim Acta 185(6):309

21. Tan S, Wang J, Han Q, Liang Q, Ding M (2018) A porous graphene sorbent coated with titanium(IV)-functionalized polydopamine for selective lab-in-syringe extraction of phosphoproteins and phosphopeptides. Microchim Acta 185(7):316

22. Liu H, Yang T, Dai J, Zhu J, Li X, Wen R, Yang X (2015) Hydrophilic modification of titania nanomaterials as a biofunctional adsorbent for selective enrichment of phosphopeptides. Analyst 140(19):6652–6659

23. Leitner A, Sakeye M, Zimmerli CE, Smatt J-H (2017) Insights into chemoselectivity principles in metal oxide affinity chromatography using tailored nanocast metal oxide microspheres and mass spectrometry-based phosphoproteomics. Analyst 142(11):1993–2003

24. Hong Y, Pu C, Zhao H, Sheng Q, Zhan Q, Lan M (2017) Yolk-shell magnetic mesoporous TiO2 microspheres with flowerlike NiO nanosheets for highly selective enrichment of phosphopeptides. Nanoscale 9(43):16764–16772

25. Li Y, Xu X, Qi D, Deng C, Yang P, Zhang X (2008) Novel Fe3O4@TiO2 core-shell microspheres for selective enrichment of phosphopeptides in phosphoproteome analysis. J Proteome Res 7(6):2526–2538

26. Ma WF, Zhang Y, Li LL, You LJ, Zhang P, Zhang YT, Li JM, Yu M, Guo J, Lu HJ (2012) Tailor-made magnetic Fe3O4@mTiO2 microspheres with a tunable Mesoporous Anatase Shell for highly selective and effective enrichment of Phosphopeptides. ACS Nano 6(4): 3179–3188

27. Yao J, Wang J, Sun N, Deng C (2017) One-step functionalization of magnetic nanoparticles with 4-mercaptophenylboronic acid for a highly efficient analysis of N-glycopeptides. Nanoscale 9(41): 16024–16029

28. Wang Y, Hai X, E S CM, Yang T, Wang J (2018) Boronic acid functionalized g-C3N4 nanosheets for ultrasensitive and selective sensing of glycoprotein in the physiological environment. In: Nanoscale

29. Jin S, Liu L, Zhou P (2018) Amorphous titania modified with boric acid for selective capture of glycoproteins. Microchim Acta 185(6): 308

30. Ma W, Xu L, Li Z, Sun Y, Bai Y, Liu H (2016) Post-synthetic modification of an amino-functionalized metal-organic framework for highly efficient enrichment of N-linked glycopeptides. Nanoscale 8(21):10908–10912

31. Jiang B, Wu Q, Deng N, Chen Y, Zhang L, Liang Z, Zhang Y (2016) Hydrophilic GO/Fe O /au/PEG nanocomposites for highly selective enrichment of glycopeptides. Nanoscale 8(9):4894–4897

32. Sun N, Wang J, Yao J, Deng C (2017) Hydrophilic Mesoporous silica materials for highly specific enrichment of N-linked Glycopeptide. Anal Chem 89(3):1764–1771

33. Zhang Y, Zhuang Y, Shen H, Chen X, Wang J (2017) A super hydrophilic silsesquioxane-based composite for highly selective adsorption of glycoproteins. Microchim Acta 184(4):1037–1044

34. Callan JF, Mulrooney RC (2009) Luminescent detection of cu(II) ions in aqueous solution using CdSe and CdSe-ZnS quantum dots functionalised with mercaptosuccinic acid. Phys Status Solidi 6(4): 920–923

35. Xu Y, Bailey UM, Punyadeera C, Schulz BL (2014) Identification of salivary N-glycoproteins and measurement of glycosylation site occupancy by boronate glycoprotein enrichment and liquid chromatography/electrospray ionization tandem mass spectrometry. Rapid Commun Mass Spectrom 28(5):471–482

36. Yao J, Sun N, Wang J, Xie Y, Deng C, Zhang X (2017) Rapid synthesis of titanium(IV)-immobilized magnetic mesoporous silica nanoparticles for endogenous phosphopeptides enrichment. Proteomics 17(8):1600320